Search for Trapped Antihydrogen: First Candidate Events

R. Hydomako, G.B. Andresen, M.D. Ashkezari, M. Baquero-Ruiz, W. Bertsche, P.D. Bowe, C.C. Bray, E. Butler, C.L. Cesar, S. Chapman, M. Charlton, J. Fajans, T. Friesen, M.C. Fujiwara, D.R. Gill, J.S. Hangst, W.N. Hardy, R.S. Hayano, M.E. Hayden, A.J. Humphries, S. Jonsell, L. V Jørgensen, L. Kurchaninov, R. Lambo, N. Madsen, S. Menary, P. Nolan, K. Olchanski, A. Olin, A. Povilus, P. Pusa, F. Robicheaux, E. Sarid, S. Seif El Nasr-Storey, D.M. Silveira, C. So, J.W. Storey, R.I. Thompson, D.P. van der Werf, D. Wilding, J.S. Wurtele, Y. Yamazaki
(ALPHA Collaboration, CERN)

Introduction

Antihydrogen, the bound state of an antiproton and position, is the simplest antiatomic system. Moreover, antihydrogen can be directly compared to hydrogen as a stringent *CPT* test.

The ALPHA (Antihydrogen Laser PHysics Apparatus) project, located in the Antiproton Decelerator (AD) at CERN, is an international collaboration with the goal of magnetically confining and performing high-precision measurements on antihydrogen.

The first step towards precision measurements is the stable confinement of antihydrogen on timescales necessary for microwave or laser spectroscopy. To this end, ALPHA has constructed a novel apparatus to create and magnetically trap antihydrogen.

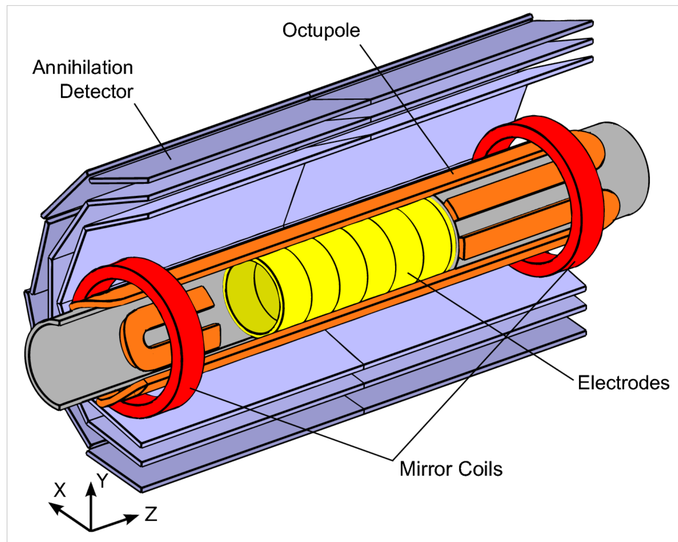

Fig. 1: Cut-away schematic of the ALPHA apparatus. Only the components relevant to the trap and detector are shown.

Experiment and Apparatus

The ALPHA apparatus combines a Penning trap for charged particles with a magnetic octupole to confine neutral antihydrogen (Fig. 1).

A strong axial magnetic field provides axial confinement of the positrons and antiprotons. The charged particles are then manipulated with an electric potential applied via the trap electrodes. The two species are brought together to form antihydrogen in the center of the magnetic neutral atom trap.

While the neutral trap is engaged, an electric field is applied to the trap volume to ensure that no charged particles remain. The neutral trap can then be quickly ramped down to reveal anything which had remained magnetically trapped inside.

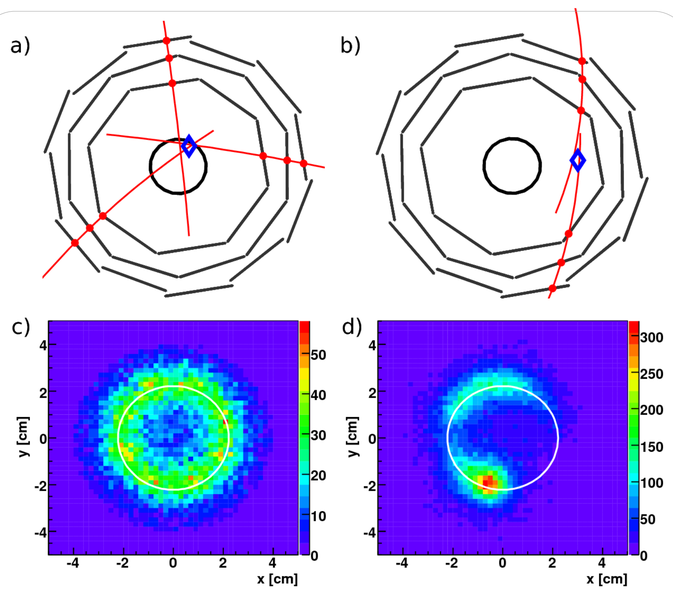

Fig. 2: (a) an example antihydrogen annihilation reconstruction, (b) example cosmic ray event reconstruction (c) X-Y cross-section of the distribution of antihydrogen annihilations (d) X-Y cross-section of the distribution of bare antiproton annihilations.

Event Reconstruction

To detect and study the antihydrogen produced, ALPHA has surrounded the trapping volume with a tracking detector. This detector (shown in Fig 1, 2a, 2b) consists of 60 double-sided silicon microstrip modules, positioned radially in three layers around the neutral trap volume.

In our case, we are interested in the primary antiproton annihilation position (vertex). As shown in Fig. 2a, this vertex can be determined by extrapolating the trajectories of two or more tracks (mostly charged pions) back to a common position.

However, annihilations are not the only events seen in our detector. Cosmic ray events (Fig. 2b) are a significant source of background. To this end, cuts on the event reconstruction parameters (Fig. 3) were carefully chosen, resulting in a final cosmic rate of 2.2 x 10^{-2} Hz.

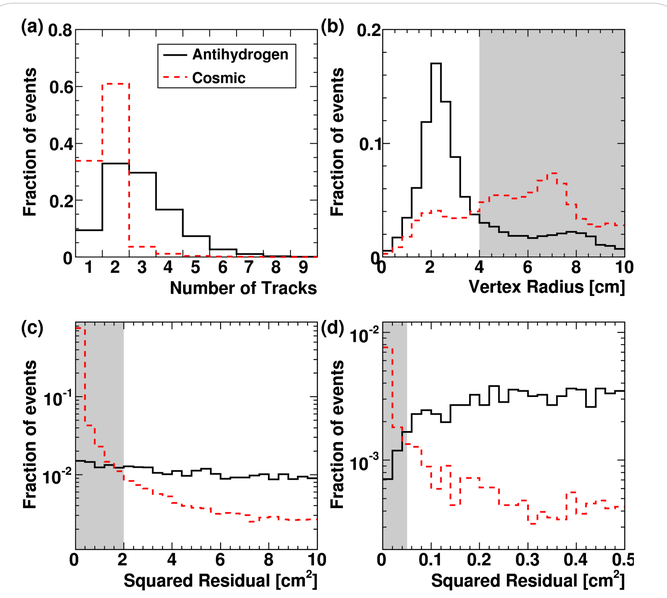

Fig. 3: The measured distributions of (a) charged particle tracks, (b) radial coordinate of the reconstructed vertex, and the squared residual from a linear fit the event hit positions for (c) two tracks, (d) more than two tracks. The cuts on the parameters are indicated but the shaded area, which shows the rejected region.

Candidate Events, Backgrounds, and Comparison to Simulations

During the 2009 experimental run, 212 trapping experiments (cycles of producing antihydrogen in the neutral trap, then ramping down the magnets to look for confined antiatoms) were performed. From these experiments, 6 candidate events, satisfying all of the cuts in Fig. 3, were observed. This is compared to an expected number of background events of 0.14. Thus, we find the p-value for the rejection of the background hypothesis of 9.2×10^{-9}, or 5.6σ. Some properties of these candidate events are summarized in Fig. 4 and Fig. 5.

It is important to note that, in addition to antihydrogen, bare antiprotons can also be confined within the neutral trap and result in an annihilation signal in the detector. Although an pulsed electric field is applied to clear away the charged particles, antiprotons with large transverse energies can remain mirror trapped in the neutral trap magnetic field.

To investigate the difference between trapped antihydrogen and mirror-trapped antiprotons, extensive simulations were performed. Fig. 5a shows the simulated distribution (in grey) of mirror-trapped antiprotons after the neutral trap ramp-down, while Fig. 5b shows the corresponding distribution for simulated antihydrogen atoms. The 6 candidate events are shown in blue. These simulated distributions strongly indicate that the candidate events are indeed trapped antihydrogen. However, without adequate validation of the simulations and an unambiguous control experiment, we cannot definitively claim to have observed trapped antihydrogen.

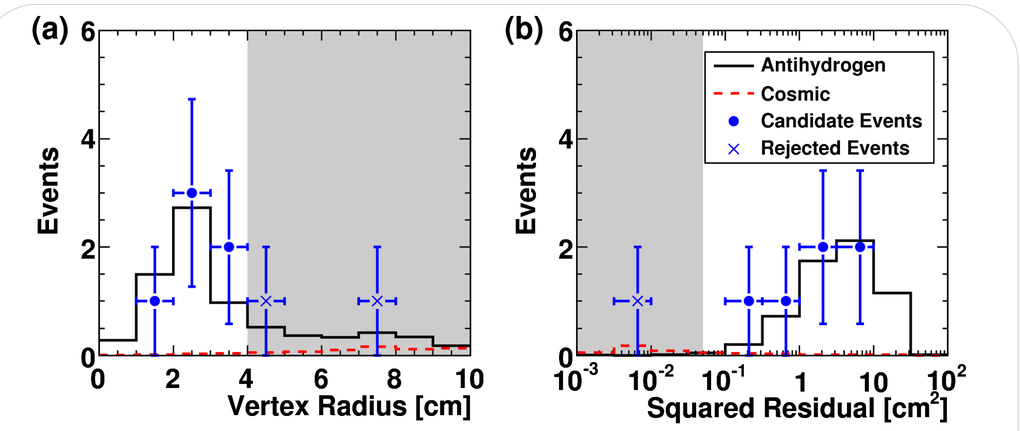

Fig. 4: Comparisons of the distributions of (a) reconstructed vertex radius, and (b) squared residuals for events in the trapping experiment and events in the calibration data set.

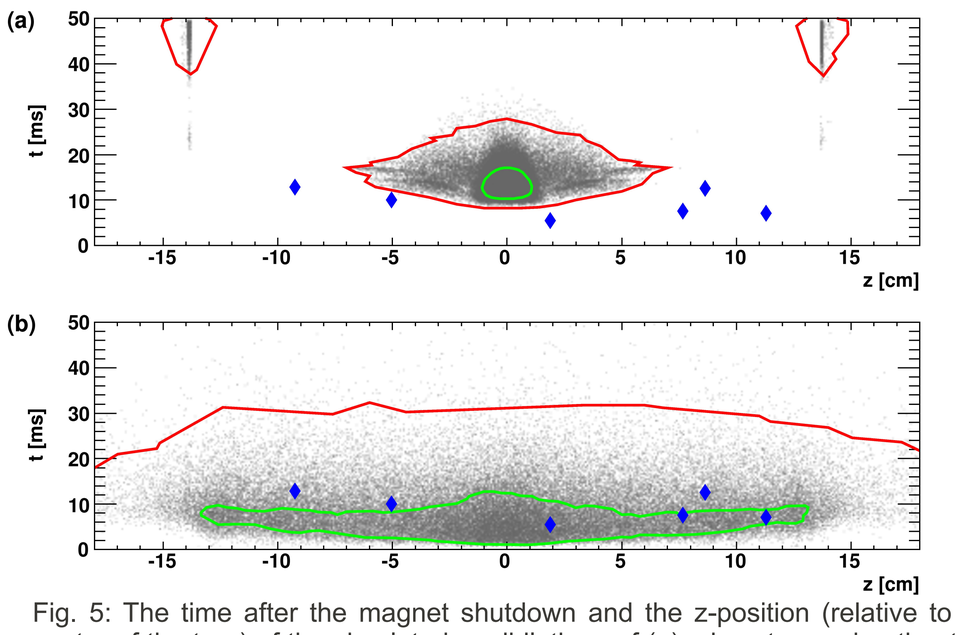

Fig. 5: The time after the magnet shutdown and the z-position (relative to the center of the trap) of the simulated annihilations of (a) mirror-trapped antiprotons and (b) antihydrogen atoms. The green contour contains 50% of the simulated events, while the red contour contains 99%. The six candidate events are shown as the blue diamonds.

Future Measurements

With the possibility of trapped antihydrogen in our apparatus, we might start thinking about the next stage of the experiment, that is, the spectroscopy of trapped antihydrogen.

A possible scheme involves using microwave radiation to induce a spin-flip in a trapped antihydrogen atom (Fig. 6), resulting in a transition from a low-field seeking state into a high-field seeking state. The atoms would no longer be magnetically confined, and would leave the trap, where the annihilation could be observed by our detector. These hyperfine transitions are well-known for hydrogen, and the comparison of the zero-field hyperfine splitting could be made in our apparatus to 1 part in 10^6.

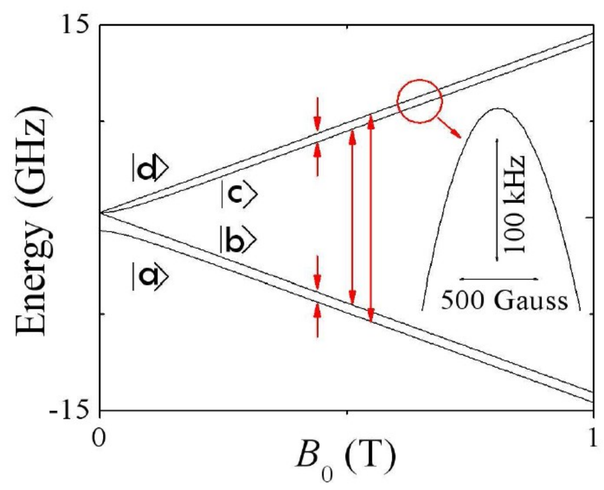

Fig. 6: Briet-Rabi diagram of the ground state of the hydrogen atom. The high-field seeking states are shown as a and b, while the low-field seeking stats are c and d. The inset shows the frequency turnaround for the c-d transition at **B**=0.65T.

Acknowledgments
This work was supported by CNPq, FINEP/RENAFAE (Brazil), ISF (Israel), MEXT (Japan), FNU (Denmark), VR (Sweden), NSERC, NRC/TRIUMF, AIF (Canada), DOE, NSF (USA), EPSRC and the Leverhulme Trust (UK).

Presenting author: rhydomako@phas.ucalgary.ca